UV-VIS and TEM assessment of morphological features of silver nanoparticles from phosphate glass matrices

Lucian Baia* **and Simion Simon**

Faculty of Physics, Babes-Bolyai University, M. Kogalniceanu 1, 400084 Cluj-Napoca, Romania

UV–VIS spectroscopy is applied to study the structural and especially morphological particularities of silver nanoclusters-phosphate glass composites from the dispersed phase perspective. The electronic absorption measurements performed on several types of phosphate glasses with different Ag_2O content indicate the existence of both silver nanoparticles of various dimensions and shapes, and Ag^+ ions, inside the glass matrix, depending on the silver oxide content. The correlation of the UV-VIS spectral results with those derived from the TEM images analysis provides further insights into the silver nanoclusters morphology. By using the experimental UV–VIS data and a theoretical approach important structural and morphological parameters, such as the radius of the silver nanospheres and the volume fraction of the spheres are determined for one of the investigated composites. The obtained radius value is in good agreement with that found from the TEM measurements.

Keywords UV-VIS spectroscopy; TEM; silver nanoparticles;

1. Introduction

In the last years because of their physical, chemical and biological properties the development of composite materials with potential in electronic, optic and biomedical applications has attracted much interest. By surveying the notable achievements in the improvement of novel photonic materials one remarks the importance of obtaining metal particles or nanoclusters embedded in glass matrices. Such composite materials have been found to exhibit desired third order optical non-linearity, which makes them promising candidates for applications in integrated optics, photonics [1-4] and ultrafast all-optical switches [5]. On the other hand, the addition of silver into the bioactive glass composition is aimed to minimize the risk of microbial contamination by taking the benefit of the potential antimicrobial activity of the leaching Ag^+ ions [6, 7]. Therefore, one of the main attraction points in the research field of biomaterials and devices is represented by the fabrication of novel bioglass materials containing silver. One of the main advantages of composite materials resides in the possibility of combining physical properties of the constituents to obtain new structural and/or functional properties. For example, the optical properties of the composites with metallic nanoparticles as dispersed phase sensitively depend on the nanoparticles size, shape, density and spatial distribution as well as the surrounding environment of the host medium [5, 8]. Therefore, in order to achieve a desired desideratum an accurate understanding of the structural and morphological particularities of the constituents is of an utmost importance.

In this respect, in the following paragraphs we purpose to evidence the existence of both silver nanoparticles of various dimensions and shapes, and Ag^+ ions, inside of a certain phosphate glass matrix ($50P_2O_5 \cdot 30CaO \cdot 20Na_2O$), depending on the silver oxide content as well as to show how can efficiently correlate the complementary information acquired from UV–VIS spectroscopy and TEM techniques. Our further interest is to point out a simply way of getting key structural and morphological parameters related to the dispersed phase of a composite sample, such as the radius of the silver nanospheres and the volume fraction of the spheres, when the experimental UV–VIS data and a theoretical approach are efficiently used. The validity of the results obtained after applying this approach is provided by the good

*Corresponding author: e-mail: lucb@phys.ubbcluj.ro, Phone: +40 264 405300

agreement between the determined mean value of the spheres radius and that derived from TEM measurements.

2. Experimental section

Glass samples belonging to (100-x)[$50P_2O_5$·$30CaO$·$20Na_2O$]xAg_2O with $0 \leq x \leq 5$ were prepared using as starting materials $NH_4H_2PO_4$, $CaCO_3$, Na_2CO_3·$10H_2O$ and Ag_2O of reagent purity grade. The mixtures corresponding to the desired compositions were melted in air, in sintered corundum crucibles, in a Carbolite RF 1600 electric furnace at 1200 °C, and maintained for 15 minutes at this temperature. The melts were quickly cooled at room temperature by pouring and pressing between two stainless steel plates [9, 10].

The UV–VIS absorption spectra were recorded on a Cary 5000 UV–VIS–NIR spectrometer with a spectral resolution of 2 nm.

A JEOL JEM 1010 transmission electron microscope (TEM) was used to evidence the presence of silver nanoparticles inside the glass matrix. Prior performing TEM measurements the glass samples were dissolved in HF and sonicated. The resulted suspensions were well washed with distilled water and deposited on a holey carbon film supported by a copper grid.

3. Results and discussion

The close analysis of the composites matrix structure, which is represented in this particular case by a soda-calcium-phosphate glass, is undoubtedly an essential point in the overall understanding of the complex structure of a composite material besides those of the structural elucidation of the constituent components and/or the linkages between them. However, since in this work our attention is exclusively directed toward evidencing structural and morphological investigation possibilities of the dispersed phase of silver particles by employing UV-VIS spectroscopy and TEM techniques, the structural particularities of the phosphate glass matrix or of the linkages between constituent components of the composites will not be discussed.

The UV-VIS absorption spectra of the (100-x)[$50P_2O_5$·$30CaO$·$20Na_2O$]xAg_2O samples, with $0 \leq x \leq 5$, are displayed in Fig. 1. Absorption bands can be observed only for the glass samples containing silver. Besides the pronounced silver plasmon resonances that appear between 400 and 500 nm, the electronic transitions involving the Ag^+ ion give rise to absorption bands located between 200 and 230 nm, whereas the electronic transitions of metallic Ag^0 appear in the 250-330 nm spectral range [11]. By looking at the UV-VIS spectra of two glasses with small Ag_2O content, x = 0.18 and 0.25, one can see (Fig.1a) distinct absorption signals around 230 nm due to the electronic transitions involving Ag^+ ions. The presence of silver ions within the glass matrix denotes the antimicrobial potential of these materials. For the samples containing higher Ag_2O content, x = 3 and 5, the signature of Ag^+ ions cannot be easily differentiated (Fig. 1b). Absorption signals due to the electronic transitions of metallic Ag^0 can be observed around 300 nm for glass samples with small (x = 0.25) and high (x = 3 and 5) Ag_2O content (see Fig. 1).

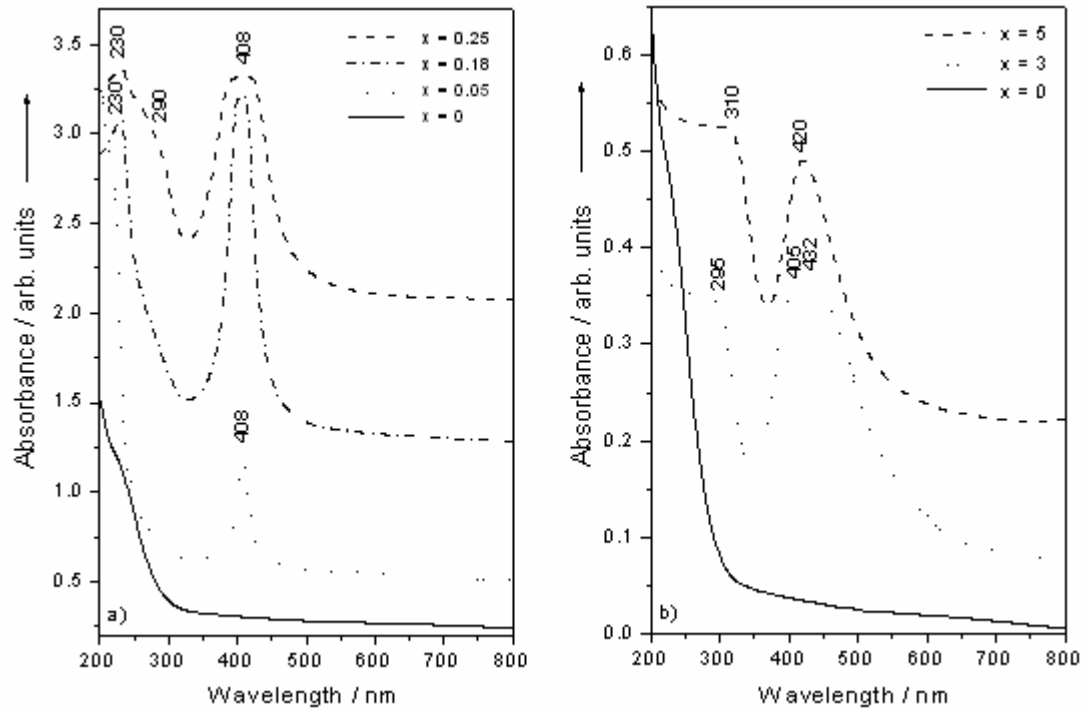

Fig. 1 UV-VIS spectra of (100-x)[$50P_2O_5 \cdot 30CaO \cdot 20Na_2O$]x$Ag_2O$ glasses for different x-values as indicated. a) small and (b) high silver content [9, 10].

By inspecting the spectral domain corresponding to higher wavelength values (> 350 nm) and by comparing the spectra of silver containing samples with that of the glass matrix one observes (Fig. 1) the appearance of silver plasmon resonance bands even for very low silver concentration (x = 0.05). Their presence signalises [9, 10, 12, 13] the existence of silver nanoparticles inside the glass matrix. Theoretical and experimental studies [5, 14], in which the optical properties of silver particles embedded in a glass matrix have been discussed evidenced the appearance in the electronic absorption spectrum of a band located at 396 nm, associated with the presence of small spherical silver nanoparticles. If the particles would not be spherical (or equiaxial), the absorption band would appear at longer wavelengths and would gradually shift to shorter wavelengths as the particles become more spherical [5, 9]. Because the position of the electronic absorption bands shown in Fig. 1a is close to the above-mentioned value we assume that the particles within the phosphate glass matrix have a roughly spherical shape [9].

A theoretical approach was further applied to determine the dimension of the silver particles. Thus, the optical absorption coefficient α of a collection of uniform silver spheres, with very small dimensions compared to the wavelength λ of the applied optical field, embedded in a medium of refractive index n, can be expressed by using the Mie scattering theory [15] in the electric dipole approximation and considering that the dielectric constant of the metal is determined by the free electrons as follows [5, 16]:

$$\alpha = \frac{9\pi p n^3 c \lambda^2}{\sigma\left[\left(\lambda_m^2 - \lambda^2\right)^2 + \lambda^2 \frac{\lambda_m^4}{\lambda_a^2}\right]} \tag{1}$$

where p, σ, c and λ_m are the volume fraction of the silver spheres in the glass matrix, the d.c. electrical conductivity, the velocity of light and the wavelength at which the maximum absorption occurs, respectively. $\lambda_a = 2\lambda^2_c\sigma/c$ and $\lambda_c = (2\pi c)^2 m/4\pi N_c \varepsilon^2_m$, m, N_c and ε_m represent the electron mass, the number of electrons per unit volume and the complex form of the dielectric constant of the silver particle, respec-

tively. By taking into account that $\lambda_m = \lambda_c\ (\varepsilon_0 + 2n^2)^{1/2}$, where ε_0 is the frequency independent part of ε_m, and that the Eq. (1) gives a band of Lorentzian shape, the full width at half maximum w of this electronic absorption band can be expressed as follows [5]:

$$w = \frac{\lambda_m^2}{\lambda_a} = \frac{\left(\varepsilon_0 + 2n^2\right)c}{2\sigma} \tag{2}$$

The d.c. conductivity σ is given by [5, 16]:

$$\sigma = \frac{\left(N_c e^2 R\right)}{mu_F} \tag{3}$$

where e is the electron charge, R the particle radius and $u_F = (2E_F/m)^{1/2}$ is the electron velocity at the Fermi energy. By replacing the expression of σ in Eq. (2) one obtains:

$$w = \frac{\left(\varepsilon_0 + 2n^2\right)cmu_F}{2N_c e^2 R} \tag{4}$$

By substituting in Eq. (4) the half-width value of the experimental absorption band recorded from the glass sample with 0.05 mol% Ag_2O (20.93 nm), $N_c e^2/m = 1.7x10^{31}$, $\varepsilon_0 = 4.9$, $u_F = 1.4x10^6$ [20,48], and by considering a refractive index of $n = 1.5$ for the glass matrix [17] a particle radius of 5.54 nm is obtained [9]. In order to ensure the validity of the above findings, related to the particles shape and their dimensions, TEM images have been recorded and are presented in Fig. 2.

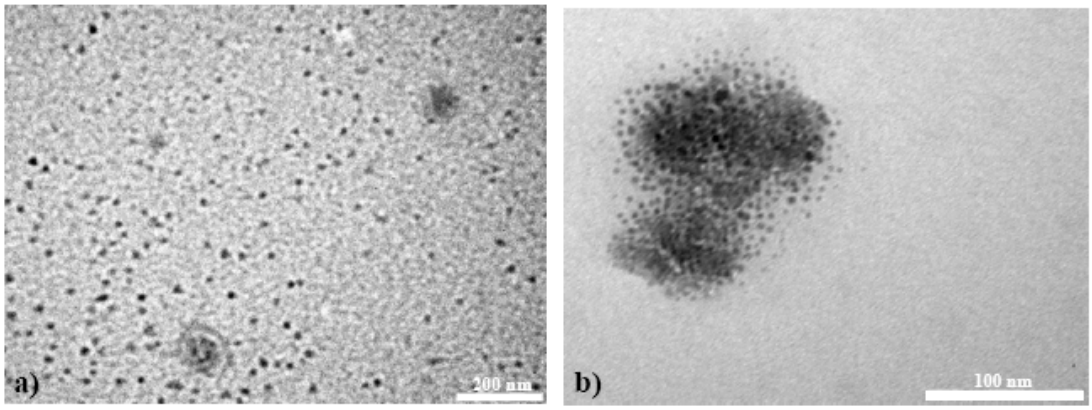

Fig. 2 TEM images of the (100-x)[$50P_2O_5$·30CaO·$20Na_2O$]xAg_2O glasses: a) x = 0.05 and b) x = 0.25 [9].

One can see that the silver particles formed within the glass sample with x = 0.05 have an almost spherical shape (see Fig. 2a) as deduced from the UV-VIS spectra analysis. A fairly good agreement between the maximum value of the silver particles size obtained from the size distribution (see Fig. 3a), as revealed by TEM images, and the calculated one (see Table 1) has been obtained [9]. The experimental and theoretical determined parameters are listed in Table 1. The UV-VIS spectra recorded on the samples with higher silver oxide concentrations, x = 0.18 and 0.25, exhibit much broader electronic absorption bands (Fig. 1a), their origin being discussed in one of the following paragraphs.

Table 1 Experimental, electronic absorption band maximum (λ_m), bandwidth (w) and sample thickness (h), and theoretical results, silver particle radius (R) and volume fraction of the silver spheres (p), obtained for the investigated glasses [9].

x [mol%]	λ_m [nm]	w [nm]	R [nm]	h (x 10^{-3}) [m]	p (x 10^{-9})
0.05	407.7	20.93	5.54	1	1.165
0.18	406	42	-	-	-
0.25	408	82	-	-	-

The electronic absorbance A can be expressed as a function of the absorption coefficient α as follows:

$$A = \alpha C h \,, \tag{3}$$

C representing the concentration of the species and h the thickness of the sample [9]. By using the absorbance measured values for the sample with the silver oxide concentration of 0.05 mol% and its thickness (see Table 1) one can represent the experimental absorption coefficient as a function of wavelength. The volume fraction of the silver spheres p, which is the only unknown value from Eq. (1), has been obtained (see Table 1) by adjusting the experimental absorption coefficient amplitude to the theoretical one. The absorption maximum, λ_m, used in Eq. (1) was the experimental value displayed in Table 1 (407.7 nm). The fairly good agreement between the experimental and theoretical absorption bands (see Fig. 4) shows the accuracy of the determined theoretical parameters.

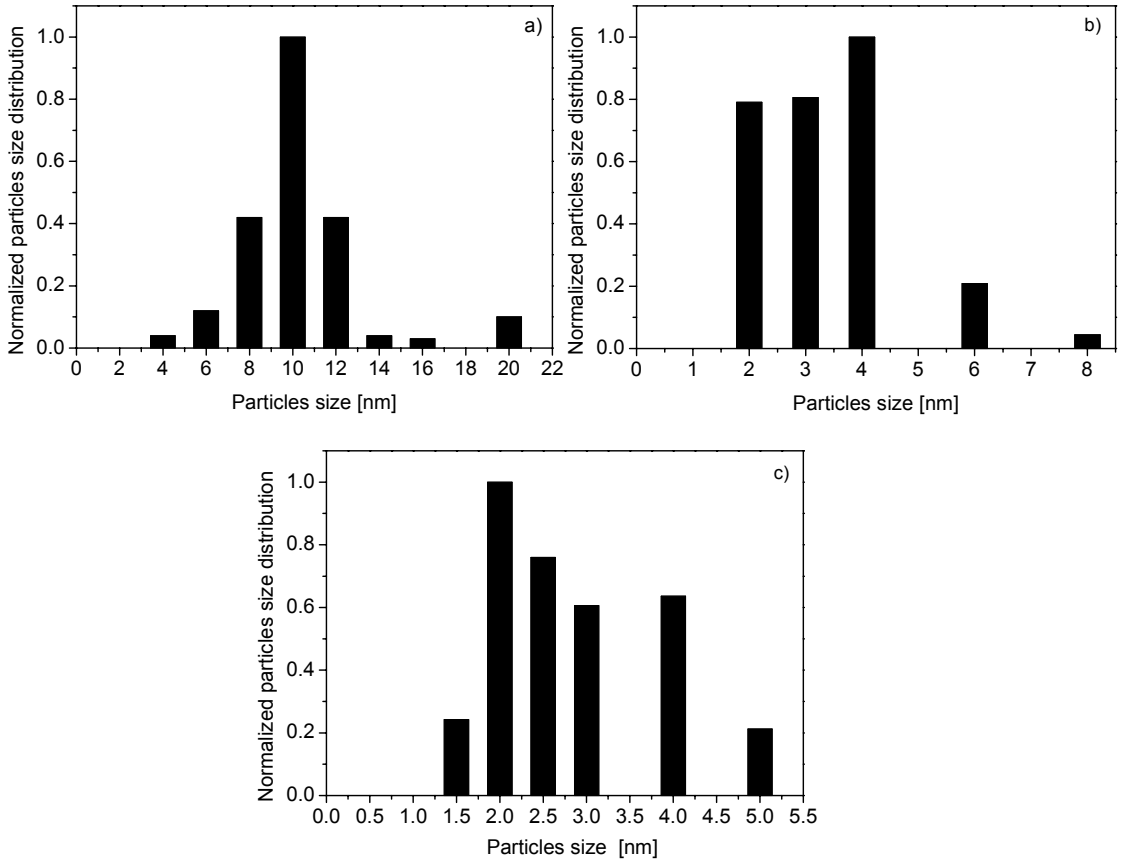

Fig. 3 Normalized size distribution of the silver nanoparticles obtained from TEM pictures analysis of the (100-x)[$50P_2O_5$·30CaO·$20Na_2O$]xAg_2O glasses with a) x = 0.05 mol%, b) x = 0.18 mol% and c) x = 0.25 mol% [9].

By inspecting the UV-VIS spectra recorded on the silver doped glasses with x = 0.18 and 0.25 one can see a gradual increase of the half-width of the electronic absorption band as the Ag_2O content becomes higher.

The dependence of bandwidth upon particle size, i.e. $w \sim 1/R$, results from the changing mean free path of the electrons [5] and shows the increase of the bandwidth with the decrease of the cluster size. The above-described theoretical approach can be applied only if the mean free path of the electrons is equal to the particle size. By looking at the bandwidth values obtained from the experimental UV-VIS spectra of the silver doped glasses for x = 0.18 and 0.25 (see Table 1) and keeping in mind the above-mentioned condition the following explanation becomes reasonable. The presence of very small nanoparticles, with radii of only a few of nanometers, is feasible for x = 0.18 and 0.25 and is responsible for the enlargement of the absorption bandwidths (Fig. 1). Having in view that the maximum value of the absorption bands is preserved, another scenario could explain their broadening. Their appearance could be caused by the presence of silver particles with the same size but with different, spherical ($< \lambda_m$) and non-spherical ($> \lambda_m$) shapes [9]. Such a broad electronic absorption band could be seen as a convolution of these bands. The TEM picture of the sample with 0.25 mol% Ag_2O (Fig. 2b) together with the sizes of the silver particles derived for the same sample (Fig. 3c) principally confirm the first hypothesis, a particles distribution of almost spherical shapes and with sizes in the range between 1.5 and 5 nm could be observed [9]. However, the second hypothesis should not be completely excluded. The mismatch between the particles ideal spherical shape and the real one from the sample with 0.05 mol% Ag_2O together with the existence of a nanoparticle sizes distribution (see Fig. 3) could account for the trivial discrepancies between theoretical and experimental values of the absorption coefficient as those observed in Fig. 4. By looking at the particles size distributions obtained from the TEM images of the composites with 0.18 and 0.25 mol% Ag_2O, which are presented in Figs. 3b and 3c, one can remark the spreading of a relatively high number of silver particles with different sizes that occurs as the Ag_2O content increases [9]. It should be also mentioned [18-21] that nanoparticles in the size range bellow 2 nm are better treated as molecular clusters and their plasmon band is strongly damped and could even disappear.

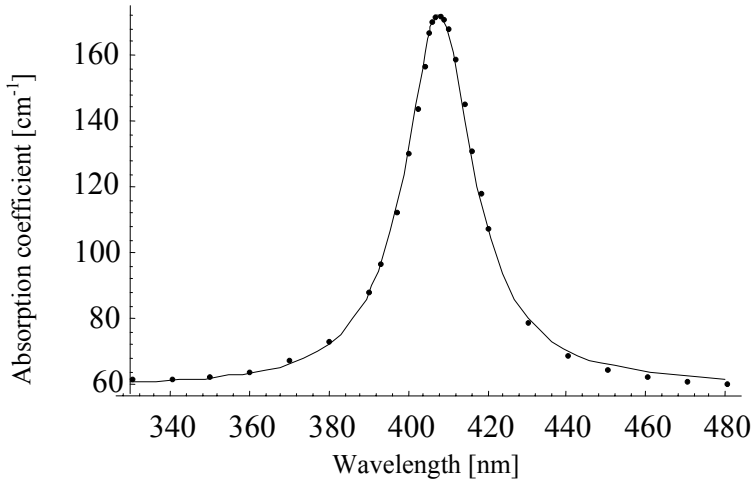

Fig. 4 (•) Measured and (—) calculated absorption band of the silver particles with radii of 5.54 nm within the $50P_2O_5 \cdot 30CaO \cdot 20Na_2O$ glass matrix [9].

The above findings related to the morphological and structural particularities of the investigated composites recommend their testing for antibacterial properties and enhancement of the non-linear response. While the first recommendation comes from the silver ions presence [22] as was mentioned before, the second one is justified as long as the enhancement of non-linear response is usually accompanied by a raising of the absorbance and consequently by the occurrence in the vicinity of the surface plasmon resonance of an increase of the third order non-linear optical susceptibility $\chi^{(3)}$, which varies roughly as $1/R$,

R representing the radius of the metal spheres [5]. Therefore, it can be assumed that these composite materials can be regarded as potential candidates for the development of new photonic materials.

In order to get further insides into the structural and morphological particularities of the composites dispersed phase with high silver content, x = 3 and 5, the spectral domains corresponding to higher wavelengths (> 350 nm) are further discussed. Concerning the optical properties of silver particles embedded in a glass matrix it was theoretically shown [5, 15] that above a certain particle size, (≈ 10 nm) the absorption band begins to shift to longer wavelengths because additional magnetic-dipole terms appear for larger radii particles. It can be thus concluded that two factors, whose influence can be monitored with the help of standard investigation techniques, mainly contribute to the shift of the plasmon resonance absorption band to higher wavelength, the particles shape and size. Nevertheless, the optical properties of the composite materials sensitively depend on many other parameters such as density and spatial distribution of the nanoparticles or the surrounding environment of the host medium. Keeping in mind the above-mentioned assertions it is justified to assume that the appearance of the absorption signal at around 405 nm in the spectrum of the sample with 3 mol% Ag_2O (Fig. 1b) is mainly due to the existence of almost spherical silver nanoparticles having small dimension within the phosphate glass matrix, while the absorption maximum at 432 nm is caused by nonspherical silver particles or/and particles with higher sizes. Similarly, the electronic absorption band at 420 nm recorded on the sample with 5 mol% Ag_2O (Fig. 1b) is most probably due to the presence of nonspherical particles or/and particles with higher sizes compared to those that give rise to the band at 405 nm, but smaller than those which are assumed to give the band at 432 nm. The appearance of less spherical nanoparticles as silver particles become higher was also previously observed [11].

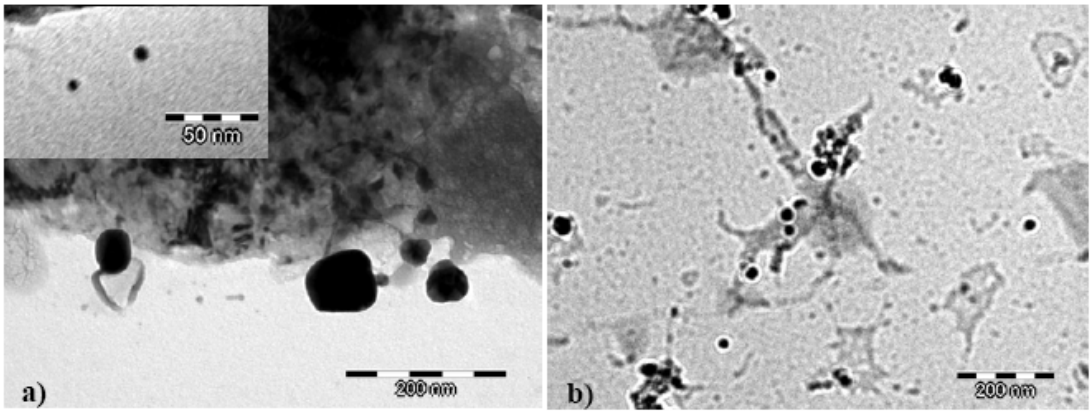

Fig. 5 TEM images of the (100-x)[$50P_2O_5 \cdot 30CaO \cdot 20Na_2O$]x$Ag_2O$ glasses: a) x = 3 and b) x = 5. The inset represents another image recorded for the sample with x = 3 at an enlarged scale [10].

TEM pictures of these two composite materials are shown in Fig. 5 and play a key role in the elucidation of the stated assumptions. In other words they clarify, complete and confirm the majority of the above considerations. Thus, for the samples containing 3 mol% Ag_2O (Fig. 5a) one can observe small nanoparticles having dimensions around 10 nm (see the inset) as well as nonspherical particles, whose length sizes are between 40 and 100 nm [10]. For the samples with the higher silver content (Fig. 5b) one can see spherical and nonspherical particles with dimensions between 20 and 40 nm. The analysis of the plasmon resonance bands intensity from the UV-VIS absorption spectrum of the sample with 3 mol% Ag_2O permits us to assume that most of the silver nanoclusters have sizes in the range 40-100 nm [10]. Thus, it is important to note the existence of particles with small dimensions for the sample with 5 mol% Ag_2O in comparison with the main part of the particles found for the sample with 5 mol% Ag_2O.

3. Conclusions

UV–VIS measurements were performed on (100-x)[$50P_2O_5 \cdot 30CaO \cdot 20Na_2O$]x$Ag_2O$ glasses, with $0 \leq x \leq 5$, in order to determine structural and morphological particularities closely related to the silver presence inside the glass matrix. The UV-VIS absorption spectra shown electronic transitions involving Ag^+ ions, especially for two from the glasses with small silver content (x = 0.18 and 0.25), this result suggesting the antimicrobial potential of these materials.

The correlation of the electronic absorption data with those derived from the TEM images analysis revealed the existence of silver nanoparticles of various dimensions and shapes, inside the composites glass matrix, depending on the silver oxide content. Important structural and morphological parameters, such as the radius of the silver nanospheres and the volume fraction of the spheres, have been determined for one of the investigated composites by using the experimental UV-VIS data in combination with a theoretical approach. The obtained radius value is in good agreement with that found from the TEM measurements.

Acknowledgements. The support by CNCSIS 1455/2007 is gratefully acknowledged.

References

[1] F. Hacke, D. Ricard, C. Flytzanis, J. Opt. Soc. Am. B **3**, 1647 (1986).
[2] R. V. Ramaswamy, H.C. Cheng, R. Srivastava, Appl. Opt. **27**, 1814 (1988).
[3] H. Hofmeister, S. Thiel, M. Dubiel, E. Schurig, Appl. Phys. Lett. **70**, 1694 (1997).
[4] P. Gangopadhyay, R. Kesavamoorthy, K.G.M. Nair, R. Dhandapani, J. Appl. Phys. **88**, 4975 (2000).
[5] P. Chakraborty, J. Mater. Science **33**, 2235 (1998).
[6] M. Bellantone, H. D. Williams, L. L. Hench, Antimicrobial Agents and Chemotherapy **46**, 1940 (2002).
[7] A. Gupta, S. Silver, Nat. Biotechnol. **16**, 888 (1998).
[8] H. Hofmeister, W.G. Drost, A. Berger, NanoStructured Materials 12 (1999) 207.
[9] L. Baia, M. Baia, W. Kiefer, J. Popp, S. Simon, Chem. Phys. **327**, 63 (2006).
[10] L. Baia, D. Muresan, M. Baia, J. Popp, S. Simon, Vib. Spectrosc. **43** (2), 313 (2007).
[11] J. Lu, J. J. Bravo-Suárez, A. Takahashi, M. Haruta, S.T. Oyama, J. Catal. **232**, 85 (2005).
[12] R. H. Doremus, J. Chem. Phys. **42,** 414 (1965).
[13] R. Yokota, K. Shimizu, J. Phys. Soc. Jpn. **12**, 833 (1957).
[14] W. Otter, Z. Physik **161,** 163 (1961).
[15] G. Mie, Ann. Phys. **225**, 377 (1908).
[16] W. Doyle, J. Phys. Rev. **111**, 1067 (1958).
[17] E. T. Y. Lee, E. R. M. Taylor, Optical Materials **28**, (200) 2006.
[18] S. Link, M. A. El-Sayed, Annu. Rev. Phys. Chem. **54**, 331 (2003).
[19]. M. M. Alvarez, J. T. Khoury, T. G. Schaaff, M. N. Shafigullin, I. Vezmer, R. L. Whetten, J. Phys. Chem. B, **101**, 3706 (1997).
[20]. T. G. Schaaff, M. N. Shafigullin, J. T. Khoury, I. Vezmer, R. L. Whetten, W. G. Cullen, P. N. First, C. Gutiérrez-Wing, J. Ascensio, M. J. Jose-Yacamán, J. Phys. Chem. B **101,** 7885 (1997).
[21] M. J. Hostetler, J. E. Wingate, C. J. Zhong, J. E. Harris, R. W. Vachet, M. R. Clark, J. D. Londono, S. J. Green, J. J. Stokes, G. D. Wignall, G. L. Glish, M. D. Porter, N. D. Evans, R. W. Murray, Langmuir, **14**, 17 (1998).
[22] D. M. Healy, T. Gilchrist, PCT Int. Appl. WO 2001028601, 2001**.**